Transient Terahertz Conductivity of GaAs Nanowires

**Patrick Parkinson,[†] James Lloyd-Hughes,[†] Qiang Gao,[‡] H. Hoe Tan,[‡]
Chennupati Jagadish,[‡] Michael B. Johnston,*,[†] and Laura M. Herz*,[†]**

University of Oxford, Department of Physics, Clarendon Laboratory, Parks Road, Oxford OX1 3PU, United Kingdom, and Department of Electronic Materials Engineering, Research School of Physical Sciences and Engineering, Institute of Advanced Studies, Australian National University, Canberra ACT 0200, Australia

Received May 17, 2007; Revised Manuscript Received June 15, 2007

ABSTRACT

The time-resolved conductivity of isolated GaAs nanowires is investigated by optical-pump terahertz-probe time-domain spectroscopy. The electronic response exhibits a pronounced surface plasmon mode that forms within 300 fs before decaying within 10 ps as a result of charge trapping at the nanowire surface. The mobility is extracted using the Drude model for a plasmon and found to be remarkably high, being roughly one-third of that typical for bulk GaAs at room temperature.

An understanding of the dynamics of charge carriers in semiconductor nanostructures is critical to the use of these materials in electronic and optoelectronic devices. In particular, semiconductor nanowires show promise as single photon detectors,[1,2] electrically driven lasers,[3] nanoscale transistors,[4] and in dye-sensitized solar cells.[5,6] Here, we determine the conductivity of photoexcited GaAs nanowires on subpicosecond to nanosecond timescales using terahertz spectroscopy. We have studied the transient photoconductivity of GaAs nanowires using a time-resolved terahertz method. Terahertz time-domain spectroscopy (THz-TDS) is an excellent probe of quasiparticle dynamics on time scales from under 1 ps to more than 1 ns.[7] To analyze carrier dynamics in semiconductors, excited species may be photoinjected into the sample using a pulse from a femtosecond laser, and the complex conductivity can be tracked using a delayed single-cycle pulse of terahertz radiation.[7] The broad bandwidth of terahertz pulses allows the characterization of the complex conductivity of a sample across a frequency range comparable to typical plasma frequencies and momentum scattering rates in semiconductors. Recent studies of nanomaterials using THz-TDS have examined silicon micro- and nanocrystals[8−10] InP and CdSe nanoparticles[11,12] and nanostructured ZnO.[13] One benefit of the THz-TDS approach is that it is noncontact and therefore avoids artefacts that may arise in purely electrical measurements from
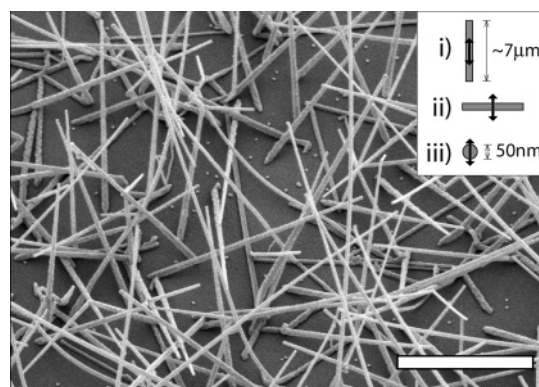

Figure 1. Scanning electron micrograph of GaAs nanowires on a quartz substrate. The scale bar (white) represents 2 μm; the image was taken at 45° to the surface. The random orientation of the nanowires is caused by the lack of symmetry of the substrate. The inset indicates three orthogonal orientations of the polarization of the terahertz electric field T. The geometrical factor f in the surface plasmon frequency is given by (i) $f = 0$ for T parallel to the axis of the nanowire, (ii) $f = 1/2$, and (iii) $f = 1/3$.

difficulties in making Ohmic contacts to a nanosized material. THz-TDS also has a range of advantages over other ultrafast techniques: for example, time-resolved photoluminescence measurements of carrier lifetimes in GaAs nanowires are hindered by a large defect density that reduces the photoluminescence efficiency.[14]

In this study, we examine GaAs nanowires grown from a gold colloid seed on a z-cut quartz substrate.[15] The scanning electron micrograph (SEM) image of the sample (Figure 1) shows an anisotropic array of nanowires with gold nanoparticles visible on the tips. An average areal density of ∼3

* Corresponding authors. E-mail: m.johnston1@physics.ox.ac.uk (M.B.J.); l.herz@physics.ox.ac.uk (L.M.H.).
† University of Oxford, Department of Physics, Clarendon Laboratory.
‡ Department of Electronic Materials Engineering, Research School of Physical Sciences and Engineering, Institute of Advanced Studies, Australian National University.
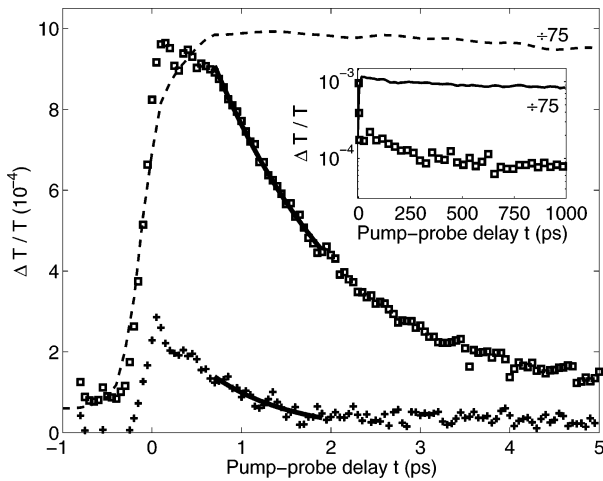
Figure 2. Pump-induced change in peak transmitted terahertz electric field ($\Delta T/T$) for different pump−probe delays t, for GaAs nanowires excited at 800 nm with an incident pump fluence of 44 μJ cm^{-2} (crosses), and 1.3 mJ cm^{-2} (squares). Solid lines indicate exponential fits, used to extract conductivity decay times shown in Figure 4g). The dashed line is for bulk GaAs at 1.3 mJ cm^{-2} but reduced in scale by a factor of 75. A weak laser pre-pulse is responsible for the nonzero $\Delta T/T$ at t < 0. Inset: $\Delta T/T$ up to $t =$ 1 ns for the nanowires (squares) and bulk GaAs (black line, ÷75) at the higher (1.3 mJ cm^{-2}) pump fluence. In both cases $\Delta T/T$ exhibits a slow exponential decay with τ > 1 ns at long delay times.

nanowires μm^{-2}, wire length of 5−10 μm, and areal fill fraction of 10 ± 2% was determined from multiple SEM images, with wire diameters of 50−100 nm. The dynamics of photoexcited electrons were measured by time-resolved THz-TDS using a setup described in the Supporting Information. Figure 2 shows the pump-induced change in the peak of the terahertz electric field pulse transmitted through the sample ($\Delta T/T$) as a function of time t after excitation. Over the first 5 ps, at an excitation-pulse fluence of 1.3 mJ cm^{-2}

(squares), the nanowires exhibit a nonexponential decay in $\Delta T/T$, which is proportional to the conductivity. In comparison, bulk GaAs has a monoexponential carrier lifetime of ~3.5 ns at the same pump fluence, as the inset to Figure 2 indicates. The substantially shorter conductivity dynamic for GaAs nanowires is a consequence of carrier trapping at surface defects and underlines their potential for use in ultrafast nanoscale optoelectronic devices. The shape of the decay in $\Delta T/T$ alters with the pump fluence, tending to a faster, monoexponential conductivity decay at lower pump fluence, as illustrated for 44 μJ cm^{-2} in Figure 2 (circles). This effect results from surface trap saturation, as discussed in more detail below.

By fixing the pump−probe delay t and recording the change in terahertz transmission, we determined the frequency-dependence of the photoinduced conductivity $\Delta\sigma(\omega, t)$ of GaAs nanowires, providing a time-resolved monitor of quasiparticle dynamics in the material. To obtain $\Delta\sigma(\omega,t)$ from $\Delta T(\omega,t)/T(\omega,t)$, we used an expression derived from standard thin-film optics. This model accounts for effects arising from the angular and size distributions of the nanowires, as explained in the Supporting Information. Figure 3 shows the extracted complex conductivity at several early pump delay times after the photoinjection of carriers. Here, the real part of $\Delta\sigma(\omega,t)$ may be thought of as the resistive response of the nanowires, with the imaginary part being associated with an additional capacitive or inductive response. During the first 200 fs after excitation, the real part of the conductivity is positive and has no discernible frequency dependence (Figure 3a). This indicates the presence of photogenerated free carriers with a large scattering rate. However, over the next 300 fs, a peak appears in the real part of the conductivity (Figure 3a), accompanied by a corresponding zero crossing in the imaginary part (Figure 3b). The frequency of this feature decreases with delay time
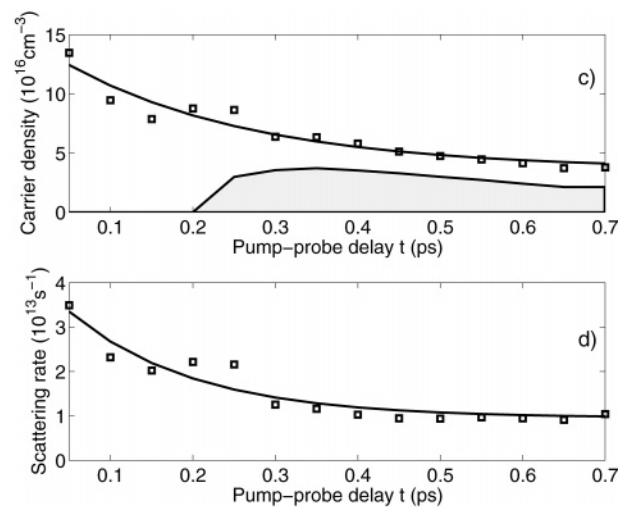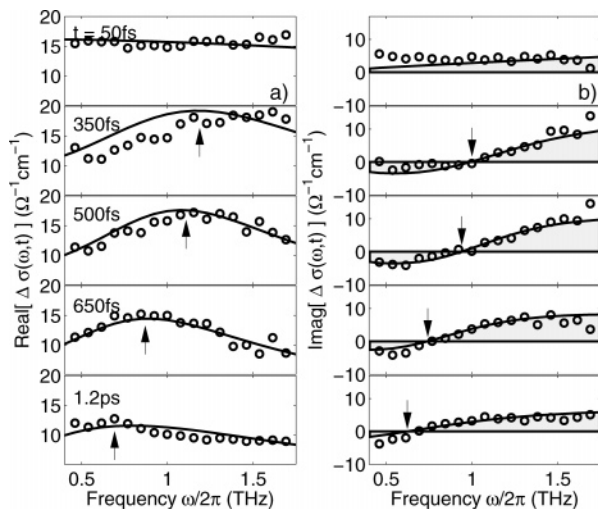

Figure 3. Time-resolved conductivity of photoexcited electrons, and the carrier density and scattering rate extracted from the plasmon model described in the text. The (a) real and (b) imaginary components of the conductivity are given at a series of pump−probe delay times for an incident pump pulse fluence of 1.3 mJ cm^{-2}. The circles are the raw data and the lines are fits including both plasmon and plasma responses. The parameters extracted from these fits are shown in (c) and (d). Figure (c) gives the total carrier density $N_{plasmon} + N_{plasma}$ (squares), with an exponential fit (solid line) with time constant 270 fs drawn as a guide to the eye. The filled area is the carrier density $N_{plasmon}$ contributing to the plasmonic response. Figure (d) shows the scattering rate (squares), with an exponential decay (solid line) with time constant 178 fs.

t, and we therefore attribute it to a carrier-density dependent mode such as a localized surface plasmon (LSP)[16] rather than an excitonic transition.[17,18] At later times $t > 2$ ps, this resonance has shifted below the frequency resolution of the system, returning to a free-carrier type response at our longest accessible delay (1 ns, not shown).

Numerous models of features in $\Delta\sigma(\omega,t)$ have been proposed, including: localized surface plasmon (LSP) modes,[8] transitions between excitonic states,[17] and the Drude—Smith model, which introduces a further parameter c_n related to incomplete randomisation of carrier momentum upon scattering.[19] While the Drude—Smith model can produce comparable shapes of the frequency-dependent conductivity to the surface plasmon model (when $c_1 \sim -1$, $c_{n>1} = 0$), it would require a time-varying backscattering parameter to model our data, which has no obvious physical origin. We therefore utilize the surface plasmon approach to model the conductivity. Terahertz radiation can couple into the (normally forbidden) plasmon mode due to the narrow width (50 nm) of the nanowires and the interaction between the modes on adjacent sides of the same nanowire.[16] The emergence of collective modes such as LSPs is expected to occur for nanoparticles, where the carrier dynamics are dominated by surface effects.[8,20]

LSP modes are coherent oscillations of the electron—hole plasma, modified from the bulk plasma frequency by the interaction with the plasma/dielectric surface interface. The relationship between the carrier density N and the plasmon frequency ω_{pl} is given by $\omega_{pl}^2 = (fNe^2)/\epsilon_0\epsilon_\infty m^*$. Here, m^* is the effective electron mass, ϵ_∞ the high-frequency dielectric response of the nanowires, and f is a factor dependent upon the surface geometry and the surrounding dielectric medium.[21] For a terahertz electric field T polarized perpendicular to the axis of a cylindric nanowire in vacuum, $f = 1/2$ or $f = 1/3$ (see inset to Figure 1), while for T parallel to the nanowire's axis, $f = 0$, and the only conductivity response is due to the bulk plasma mode. The complex conductivity of a free-electron plasma with a plasmon resonance is given within the Drude framework by[8]

$$\sigma(\omega) = \frac{iNe^2\omega}{m^*(\omega^2 - \omega_{pl}^2 + i\omega\gamma)} \qquad (1)$$

where ω_{pl} is the plasmon frequency (determined by the relationship given earlier) and γ is the momentum scattering rate. For an ensemble of nanowires oriented at random angles, we expect a contribution to the photoinduced conductivity dominated by two different modes: a plasmon at ω_{pl} and the bulk plasma at $\omega_{pl} = 0$. To model the measured $\Delta\sigma(\omega,t)$, we therefore sum two contributions to the conductivity of the form given in eq 1, one with a carrier density N_{bulk} and $f = 0$ for the bulk mode and another with carrier density $N_{plasmon}$ and $f = 1/2$ (as the $f = 1/3$ mode presents negligible surface area). The scattering rate γ is assumed to be the same for both modes. Excellent fits to the measured data are obtained over the full range of pump—probe delays t, as indicated by the solid lines in Figure 3. The carrier densities and scattering rates extracted are shown as a
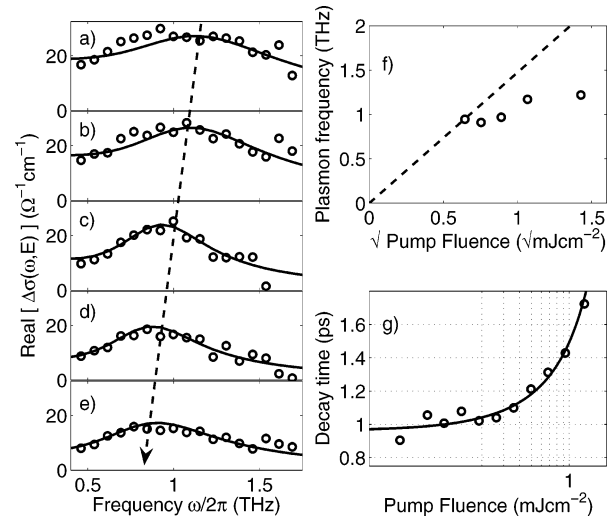
Figure 4. Pump fluence dependence of terahertz conductivity at a pump—probe delay $t = 550$ fs. Real part of photoinduced conductivity after excitation with various pump energies: (a) 2 mJ cm^{-2}, (b) 1.1 mJ cm^{-2}, (c) 0.79 mJ cm^{-2}, (d) 0.57 mJ cm^{-2}, and (e) 0.42 mJ cm^{-2}, where points are raw data and solid lines are from the model described in the text. Figure (f) shows the extracted plasmon frequency ω_{pl} as a function of pump fluence F (circles) in comparison with a prediction from $\omega_{pl} \propto \sqrt{F} \propto \sqrt{N}$. Figure (g) gives the lifetime of the conductivity as a function of incident pump fluence extracted from exponential fits to a series of pump—probe delay scans. The rate equation model described in the text (solid line) accurately reproduces the fluence dependence of the carrier lifetime.

function of pump—probe delay in parts c and d of Figure 3, respectively. While the carrier density in the bulklike mode is observed to form rapidly, that in the plasmon mode has only built up after 300 fs. In bulk GaAs, the free-electron plasma response develops over a time scale comparable with the inverse of the plasma frequency.[22] The plasmon frequency is lower than that of the plasma, consistent with the observed longer formation time for the nanowires. In Figure 3d, the scattering rate can be seen to decrease initially with t before remaining roughly constant at 10^{13} s^{-1} for $t > 400$ fs. From the extracted scattering rates, we determine the charge carrier mobility μ in the long-time limit within the Drude model ($\mu = em^{*-1}\gamma^{-1}$) to be 2600 cm^2 V^{-1} s^{-1}. Remarkably, this value is only a factor of 3 lower than typical electron mobilities in bulk GaAs at room temperature,[23] highlighting the prospect of implementation of these structures in fast nanoscale electronics.

The observed drop in the carrier density with time is indicative of the ultrafast trapping or decay of the surface carrier population. An experiment using a fixed pump—probe delay ($t = 550$ fs) and a range of incident pump fluences F was carried out to allow comparison between plasmon frequencies ω_{pl} deduced from experiment with those anticipated assuming linearity between the pump fluence and photoexcited carrier density. The plasma frequencies extracted from fits to the conductivity spectra (Figure 4a—e) using the previously discussed model are plotted in Figure 4f) as a function of pump fluence. While the plasmon frequency increases with pump fluence, it does not scale according to $\omega_{pl} \propto \sqrt{F} \propto \sqrt{N}$. This suggests that the

photoexcited carrier density in the first 550 fs is nonlinear with respect to fluence. Such behavior may be expected, as either band-filling or ultrafast trapping within the first 550 fs can lead to a saturation of carriers that are able to take part in the collective surface mode.

As surface trapping strongly affects the carrier lifetime, it is essential to obtain an estimate of the surface trap density in order to calculate the carrier density at which saturation has an effect. To investigate this behavior, monoexponential curves were fitted to a range of pump−probe scans over the time window $t = 0.8-1.8$ ps (see Figure 2), with the resulting decay times shown in Figure 4g. A clear dependence of the carrier relaxation time on pump fluence can be seen, with a doubling in the trapping time τ when the incident pump fluence is increased 30-fold. As the mobility remains constant over the examined time interval, this change is primarily due to saturation of the surface traps by the large photoinduced carrier population, leading to a reduction in available trap states with increasing pump fluence. For a more quantitative analysis, these data were fitted with the numerical solution of a rate equation for carrier trapping[9] that included a finite number of available traps and yielded a trap density of $N_{traps} = 2 \times 10^{17}$ cm^{-3} and a trapping cross-section of 6×10^{-14} cm^2 (solid line in Figure 4g). The extracted trap density is comparable to the initial photoinjected carrier density, explaining the distinct change in carrier lifetime with pump fluence as the carrier density passes this mark.

In conclusion, we have measured the transient terahertz conductivity of GaAs nanowires on subpicosecond to nanosecond time scales using a noncontact optical probe based on time-domain spectroscopy. The observed conductivity dynamics differ strongly from those for bulk GaAs, displaying ultrashort ($\sim$1 ps) lifetimes that depend critically on the trap density at the nanowire surface. These results open the possibility for implementation of these nanowires in ultrafast switching devices, whose properties can be optimized through a multitude of mechanisms such as overcoating the nanowires with a higher band gap material[14,24] or chemical passivation of surface defects.[25] The electron mobility for the nanowires at room temperature was extracted from the data by modeling of the plasmon resonance that forms within the first 300 fs after excitation. The resulting value of 2600 cm^2 V^{-1} s^{-1} is only a factor of 3 lower than that typical for bulk GaAs, demonstrating that high-quality epitaxial growth can generate nanowires with excellent electronic properties.

References

(1) Fujiwara, A.; Yamazaki, K.; Takahashi, Y. *Appl. Phys. Lett.* **2002**, *80*, 4567−4569.

(2) Robinson, B. S.; Kerman, A. J.; Dauler, E. A.; Barron, R. O.; Caplan, D. O.; Stevens, M. L.; Carney, J. J.; Hamilton, S. A.; Yang, J. K. W.; Berggren, K. K. *Opt. Lett.* **2006**, *31*, 444.

(3) Duan, X. F.; Huang, Y.; Agarwal, R.; Lieber, C. M. *Nature* **2003**, *421*, 241.

(4) Cui, Y.; Zhong, Z.; Wang, D.; Wang, W. U.; Lieber, C. M. *Nano Lett.* **2003**, *3*, 149−152.

(5) Dittmer, J. J.; Marseglia, E. A.; Friend, R. H. *Adv. Mater.* **2000**, *12*, 1270−1274.

(6) Kim, Y.; Choulis, S. A.; Nelson, J.; Bradley, D. D. C.; Cook, S.; Durrant, J. R. *Appl. Phys. Lett.* **2005**, *86*, 063502.

(7) Schmuttenmaer, C. A. *Chem. Rev.* **2004**, *104*, 1759−1779.

(8) Nienhuys, H. K.; Sundstrom, V. *Appl. Phys. Lett.* **2005**, *87*, 012101.

(9) Jepsen, P. U.; Schairer, W.; Libon, I. H.; Lemmer, U.; Hecker, N. E.; Birkholz, M.; Lips, K.; Schall, M. *Appl. Phys. Lett.* **2001**, *79*, 1291−1293.

(10) Cooke, D. G.; MacDonald, A. N.; Hryciw, A.; Wang, J.; Li, Q.; Meldrum, A.; Hegmann, F. A. *Phys. Rev. B* **2006**, *73*, 193311.

(11) Beard, M. C.; Turner, G. M.; Murphy, J. E.; Micic, O. I.; Hanna, M. C.; Nozik, A. J.; Schmuttenmaer, C. A. *Nano Lett.* **2003**, *3*, 1695−1699.

(12) Beard, M. C.; Turner, G. M.; Schmuttenmaer, C. A. *Nano Lett.* **2002**, *2*, 983−987.

(13) Baxter, J. B.; Schmuttenmaer, C. A. *J. Phys. Chem. B* **2006**, *110*, 25229−25239.

(14) Titova, L. V.; Hoang, T. B.; Jackson, H. E.; Smith, L. M.; Yarrison-Rice, J. M.; Kim, Y.; Joyce, H. J.; Tan, H. H.; Jagadish, C. *Appl. Phys. Lett.* **2006**, *89*, 173126.

(15) Kim, Y.; Joyce, H. J.; Gao, Q.; Tan, H. H.; Jagadish, C.; Paladugu, M.; Zou, J.; Suvorova, A. A. *Nano Lett.* **2006**, *6*, 599−604.

(16) Zayats, A. V.; Smolyaninov, I. I. *J. Opt. A: Pure Appl. Opt.* **2003**, *5*, S16−S50.

(17) Kaindl, R. A.; Carnahan, M. A.; Hagele, D.; Lovenich, R.; Chemla, D. S. *Nature* **2003**, *423*, 734.

(18) Wang, X.-L.; Voliotis, V. *J. Appl. Phys.* **2006**, *99*, 121301.

(19) Smith, N. V. *Phys. Rev. B* **2001**, *64*, 155106.

(20) Bryant, G. W.; Jaskolski, W. *J. Phys. Chem. B* **2005**, *109*, 19650−19656.

(21) Pitarke, J. M.; Silkin, V. M.; Chulkov, E. V.; Echenique, P. M. *Rep. Prog. Phys.* **2007**, *70*, 1−87.

(22) Huber, R.; Tauser, F.; Brodschelm, A.; Bichler, M.; Abstreiter, G.; Leitenstorfer, A. *Nature* **2001**, *414*, 286−289.

(23) Madelung, O., Ed.; *Semiconductors: Basic Data;* Springer: New York, 2003.

(24) Hoang, T. B.; Titova, L. V.; Yarrison-Rice, J. M.; Jackson, H. E.; Govorov, A. O.; Kim, Y.; Joyce, H. J.; Tan, H. H.; Jagadish, C.; Smith, L. M. *Nano Lett.* **2007**, *7*, 588−595.

(25) Lloyd-Hughes, J.; Merchant, S. K. E.; Lan, F.; Tan, H. H.; Jagadish, C.; Castro-Camus, E.; Johnston, M. B. *Appl. Phys. Lett.* **2006**, *89*, 232102.

NL071162X